

Synthesis and optical properties of CdS nanowires by a simple chemical deposition

Ying Zhao · Xiu-chun Yang · Wen-hai Huang ·
Xiao Zou · Zhen-guang Lu

Received: 10 August 2009 / Accepted: 22 December 2009 / Published online: 5 January 2010
© Springer Science+Business Media, LLC 2010

Abstract CdS nanowires were prepared by a paired cell method, using highly ordered porous anodic alumina (PAA) membranes as templates. The morphology, structure, and composition of these nanowires were characterized by scanning electron microscopy (SEM), high-resolution transmission electron microscopy (HRTEM), energy dispersive X-ray spectroscopy (EDS), and selected area electron diffraction (SAED) pattern. SEM images indicated that nanowires arrays are highly ordered and coincide with the contours of PAA. The EDS analysis, combined with HRTEM images and SEAD patterns, confirmed the formation of CdS. The formation and growth mechanism of CdS nanowires, as well as the optical properties, were also analyzed in details. The results indicated that the formation and growth of CdS nanowires experience from initial nuclei, nanoparticles, linear pearl-chain structures to final nanowires, attributed to electrostatic adsorption and ions diffusion. A strong emission with a maximum around 430 nm was observed from the synthesized CdS nanowires, which was attributed to the recombination of trapped electron/hole pairs. The absorption edge in UV–Vis spectrum of CdS/PAA nanoarrays showed a blue shift due to the quantum confinement effects. The technique can be used to fabricate other compound nanowires and newly light-emitting semiconductor materials.

Introduction

CdS is one of the most important II–VI group semiconducting and optoelectric material, and has a band gap

2.42 eV at room temperature [1]. Much attention has been received due to its direct band gap resulting in emission in the visible wavelength region. Nanostructured semiconducting sulfide materials are technologically important owing to their unique optical and electronic properties, which differ from the corresponding bulk materials. Therefore, CdS nanomaterials are being widely investigated for its potential applications in solar cells [2], lasers [3], waveguides [4], field-effect transistors [5], piezoelectric nanogenerators [6], and other photoelectric devices.

It is well known that several methods have been used for the synthesis of one-dimensional CdS nanowires. Li et al. [7] synthesized CdS nanowires in hexagonal liquid crystals formed by surfactant $C_{16-18}EO_7$ (a soft template). Shi et al. [8] synthesized CdS nanowires in microemulsion system of sodium dodecylbenzene sulfonate (SDBS) through the reaction of Cd^{2+} with CS_2 in ethylenediamine. Kang et al. [9] synthesized catalyst-free CdS nanowires by using a mixture of surfactants. Wang et al. [10] and Lin et al. [11] achieved CdS nanowires by physical vapor deposition (PVD) via the vapor–solid growth mechanism under controlled conditions. Routkevitch et al. [12] and Xu et al. [13] adopted electrochemical method to fabricate CdS nanowires by depositing CdS into the pores of anodic aluminum oxide films. All of these methods are very useful and are of widespread importance, but there are some limitations to their utility, which some methods either require elevated temperature, or use toxic agent, or need significant energy input, or gain pure CdS difficultly [14].

Compared with the above-mentioned methods, the chemical deposition using a paired cell is a relatively simple, electrodeless, and low cost process for the growth of nanotubes and nanowires [15, 16]. In this paper, we investigated the synthesis of CdS nanowires in porous anodic alumina (PAA) templates via a paired cell method

Y. Zhao (✉) · X. Yang · W. Huang · X. Zou · Z. Lu
School of Materials Science and Engineering, Tongji University,
Shanghai 200092, China
e-mail: yingzhao@126.com

without employing toxic agent and energy input. Comprehensive research including nucleation, growth, and optical properties (photoluminescence, UV–Vis absorption etc.) of CdS nanowires were presented and discussed, which were not clear up to now.

Experimental

Preparation of PAA template

High-purity aluminum foil (99.999%, GRIKIN Advanced Materials Co., Ltd China) was used as the starting material for PAA template. Before anodization, the aluminum was degreased with acetone and then annealed at 500 °C for 4 h to remove mechanical stress and allow recrystallization. After electropolished in a mixture solution of 95 vol% H_3PO_4 + 5 vol% H_2SO_4 + 20 g/L Cr_2O_3 , the aluminum was anodized in a two-step anodization process [17]. The reaction was performed at constant voltage (40 V) and temperature (5 °C) in 0.3 M oxalic acid ($\text{C}_2\text{H}_2\text{O}_4$) for 10 h. After removal of the alumina layers by immersion in a mixture of 6 wt% H_3PO_4 and 1.8 wt% H_2CrO_4 at 60 °C for 10 h, the aluminum foil was anodized again for 6 h under the same anodization condition as the first step. The remaining aluminum layers at the bottom of the alumina membranes were removed in a saturated CuCl_2 solution. A transparent and through-hole alumina template was obtained by a subsequent etching treatment in 5 wt% phosphoric acid.

Preparation of CdS nanowire arrays

A paired cell was constructed using two plexiglass half-cells, which were separated by the nanoporous alumina membrane. Aqueous solutions of 0.05 M Na_2S and 0.05 M CdCl_2 were very slowly poured into each half-cell. After completion of the reaction for 2 h, the resulting CdS/PAA composite was taken out and thoroughly washed with deionized water. Additionally, some of the specimens need to be further immersed into NaOH solutions to remove alumina template and gain nanowires without the support of the template.

Instruments

The morphology and composition of the prepared membranes were examined using a scanning electron microscope (SEM, Quanta 200 FEG, FEI Company). High resolution transmission electron telescope (HRTEM, JEM-2010F TEM, Japan) was employed to characterize the structure of nanowires. Fluorescence spectrophotometer (760 CRT, Shanghai Precision & Scientific Instrument Co., Ltd) and UV–Vis spectrophotometer (FLH-466, HITACH

Company) were used to measure photoluminescence (PL) spectra and absorption spectra, respectively.

Results and discussion

SEM images of PAA membranes

Figure 1a shows a SEM top view of the PAA membranes formed via the two-step anodization process, as described previously. The alumina membranes exhibit an ideally hexagonal configuration, uniform cell size, and highly ordered pore arrangement over a large area. The thickness of the PAA membranes is about 30 μm . The pore diameter and pore density are approximately 60 nm and $1 \times 10^{10} \text{ cm}^{-2}$, respectively. And they can be easily varied by adjusting anodization parameters such as electrolyte concentration, ambient temperature, and anodizing voltage. It also can be seen in the typical side-view micrograph (Fig. 1b) that the pore channels of the as-prepared alumina membrane are well-defined, straight, with smooth inner surfaces. The structure has been proven to be suitable for the synthesis of one-dimensional nanomaterials with high-quality [18].

Morphology and structure of CdS nanowire arrays

Figure 2a shows the SEM image of the as-prepared nanowires/PAA composite. While free nanowires without the support of the PAA membranes are presented in Fig. 2b. As can be seen, the nanowires formed via the paired cell method are homogeneous, 50 nm in diameter, with a coarse outer surface. The EDS (Fig. 3) analysis reveals only cadmium and sulfur existed in the nanowires, and the ratio of cadmium atom to sulfur atom is approximately to be 1:1. It can be inferred that the nanowires are constituted by CdS. The content of Cd is more than S (an atomic ratio Cd/S of 1.3), which is probably caused from the fact that Cd^{2+} ions diffuse faster than S^{2-} ions and more Cd deposits in the pore channels, and results in a slight sulfur defect and finally nonstoichiometric CdS formation. Such sulfur deficiency seems to be typical in chemical deposited CdS [19, 20].

From Fig. 2b, it is easy to identify that the nanowires were composed of linear pearl-chain structures with the nanoparticles of about 10 nm in diameter. Although fully free CdS nanowires were somewhat coarse, individual CdS nanowire in the alumina channels was expected to have a high aspect ratio (about 1000). Additionally, it also can be seen that the average diameter of the resulting CdS nanowires was slightly less than the average pore diameter of the alumina template. This reason is probably that nanoparticles blocked the alumina channel during the reaction and further reaction was impeded.

Fig. 1 SEM images of the alumina membrane obtained by the two-step anodization process; **a** top view, **b** side view

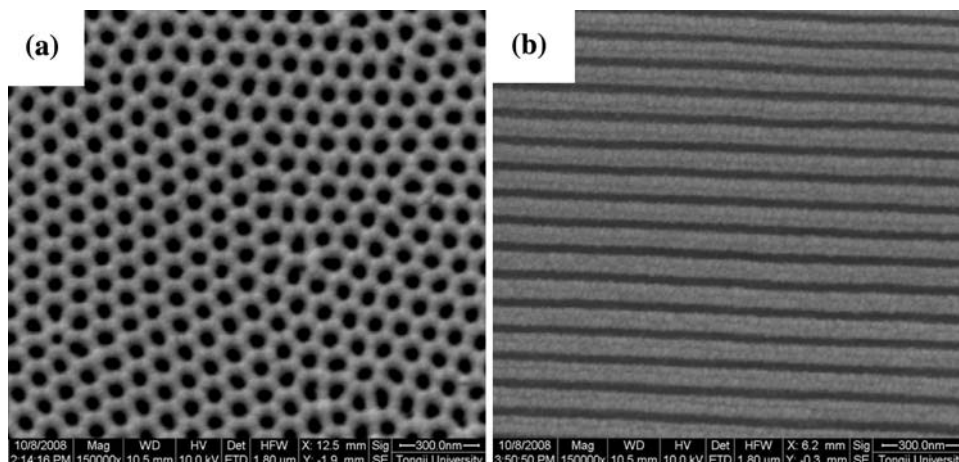


Fig. 2 SEM images of **a** CdS/PAA composite membranes (side view); **b** free CdS nanowires without the support of PAA membranes

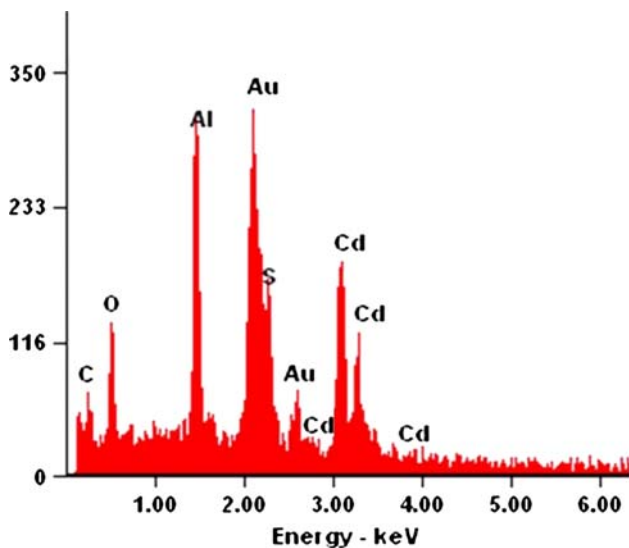
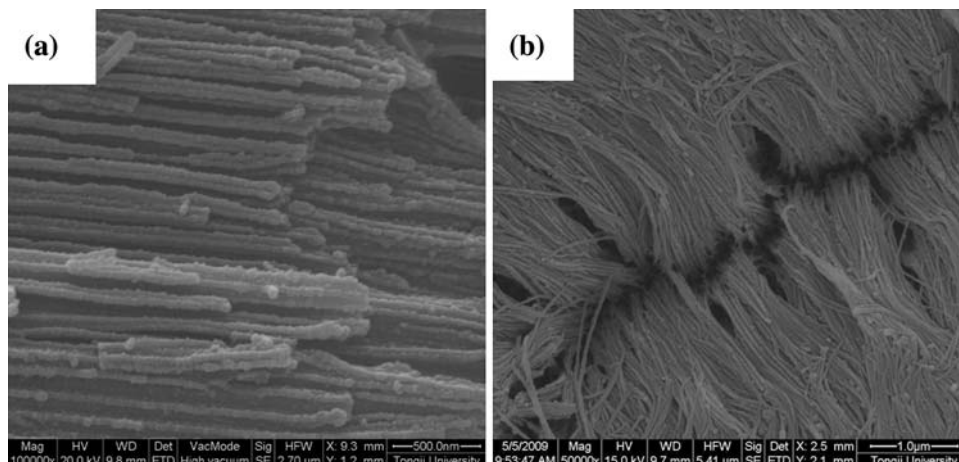


Fig. 3 EDS spectrum of as-prepared CdS/PAA composite membranes

Figure 4 shows the TEM image and the corresponding partial high resolution TEM (HRTEM) images and the selected area electron diffractions (SAED) patterns of an

as-prepared nanowire with a diameter of 50 nm. The TEM image suggests a uniform wire structure for the CdS deposit (Fig. 4a). The HRTEM images present that the as-prepared nanowire is constituted of nanoparticles of about 10 nm in diameter (Fig. 4b, c). Meanwhile, they reveal the spacings of the apparent crystallographic planes at around 0.315, 0.189, 0.245, and 0.335 nm, which are indexed as the (101), (103), (102), and (002) plane of hexagonal CdS. The SAED further demonstrate the polycrystalline CdS formation. In addition, as can be seen in the HRTEM images, some areas do not contain the lattice fringes, suggesting the existence of amorphous CdS in the nanowire. It is also resulted from defects unavoidably formed in chemical deposited CdS.

Formation mechanism of CdS nanowire arrays

According to the authors’s experimental results, a possible formation mechanism of CdS nanowire arrays is suggested. In the paired cell, CdCl₂ and Na₂S solutions are separated by porous alumina template. The experimental results showed Cd²⁺ and S²⁻ must pass through the alumina nanopores, if they diffuse and enter the other cell. In the

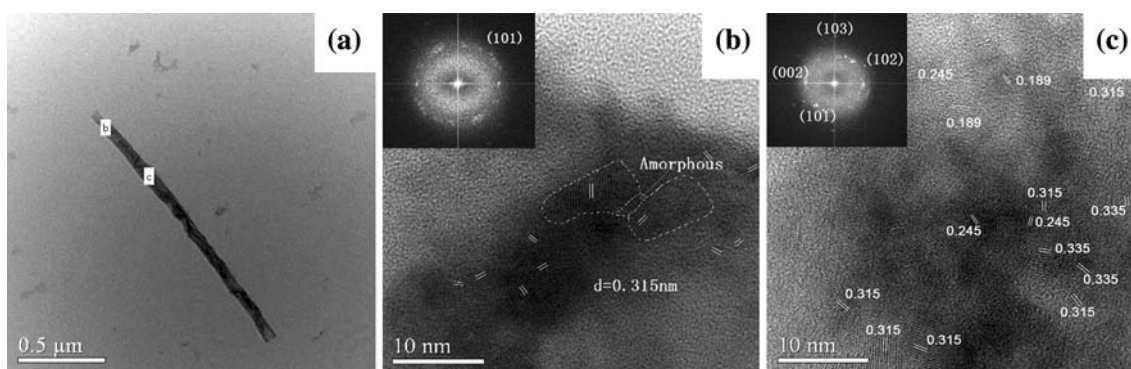


Fig. 4 TEM image (a) and the corresponding partial HRTEM images and SEAD patterns (b, c) of a CdS nanowire

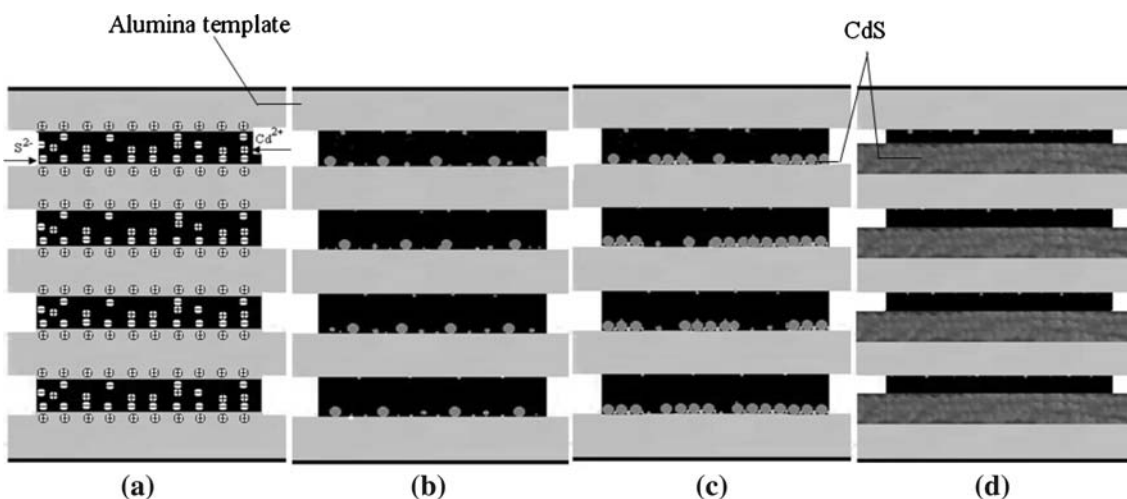
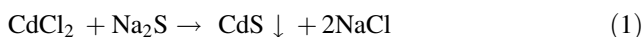


Fig. 5 Schematic diagram for the formation of CdS nanowires using paired cell

first stage, large quantity of Cd^{2+} and S^{2-} was limited inside the pores. Since the pore walls were positively charged [21], S^{2-} would be adsorbed onto the walls through electrostatic interaction. Then, Cd^{2+} reacted with S^{2-} to produce crystalline CdS nuclei on the alumina pore walls [15] (see Fig. 5). The reaction process can be expressed by Eq. 1.



This reaction can also be used to synthesis the other similar semiconductor nanowires, such as CuS, Ag_2S and AgI.

During the reaction, Cd^{2+} and S^{2-} enter the nanopores continuously from both sides. Once a nucleus has been formed at a certain location, from a free energy perspective, it is easier for the growth of the existing nucleus than the formation of new nucleus. In the stage, even though Cd^{2+} and S^{2-} meet inside the alumina nanopores, CdS nanocrystals preferentially nucleate and grow onto the pore walls in view of low nucleation energy on heterogeneous surface (Fig. 5b). As Cd^{2+} and S^{2-} enter the nanopores

continuously from both sides, the crystalline nuclei will grow and aggregate to form CdS nanoparticles. The formation kinetics of long one-dimensional nanostructures start from the primary nanoparticles. It consists of two processes: (1) the nanoparticles further aggregate to form linear pearl-chain structures, (2) coalescence of preformed nanoparticles within the chain (Fig. 5c). The two steps can take place simultaneously, or they may be separated in time if their time scales are different. The processes are preferentially performed in the bottom of alumina channel on account of gravity action. With the increase of reaction time, new nuclei are formed and grown up on the original linear pearl-chain structures, finally leading to the formation of thick nanowires (Fig. 5d).

During the crystallization of the CdS nanowires, the free energy of the system and the critical size of a stable nucleus varied on function of the reaction temperature, reagent concentration, and solid–liquid interface energy. The higher the reaction temperature, the greater is the free energy of the system. At lower reaction temperatures, the critical nuclei size as well as the energy barrier will

increase, thereby decreasing the nucleation density. In this case, only prolonging the growth time can meet the requirement of the nanowires formation. In our experiment, it took 2 h to form integrated CdS nanowires.

In the early formation of CdS nanowires, electrostatic adsorption drives the initial nucleation. With further deposition, diffusion (including internal ions diffusion in CdS and interface diffusion in CdS/PAA) begins to play an important role. The defects existing on the interface are favorable to ions diffusion, while ions diffusion slowly in the internal solid, where the interface diffusion plays a more important role.

In our research, it should be clearly noted that the growth of CdS and other sulfide nanowires by the paired cell method were not equally favored. The former is found to be more difficult, resulting in lower yields for heterostructures. The reason for this difference is not clear at present and requires further investigation.

Optical properties

Figure 6 shows the UV–Vis absorption spectrum of CdS/PAA nanoarrays. In this figure, the absorption edge of the spectrum for the nanoarrays is about 400 nm, which exhibits 120 nm shifts towards high energy with respect to the absorption edge for the bulk of 520 nm. Similar huge shift was observed in some reports [22, 23]. The blue shift of the absorption edge in UV–Vis spectrum of CdS/PAA nanoarray can be attributed to the quantum confinement effects of nanoparticles.

Figure 7 shows the PL spectra of the as-prepared CdS/PAA and PAA measured with an excitation of the 280 nm line of a Xe lamp. It can be seen that intensive PL bands appear at about 430, 460, 479, and 490 nm for CdS/PAA arrays. Compared with the PL bands of PAA, an extra

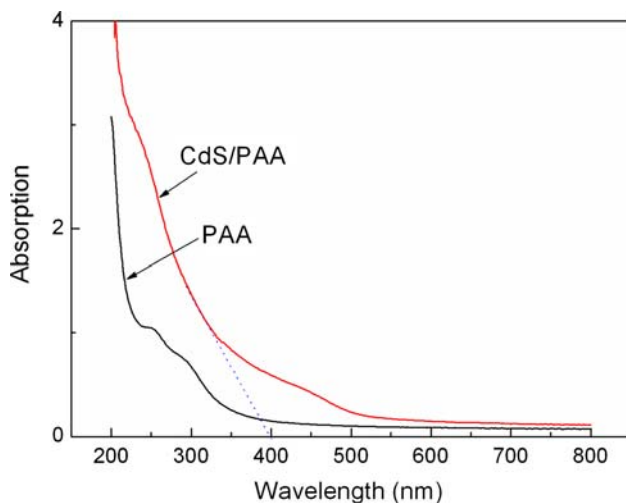


Fig. 6 UV–Vis absorption spectra of the CdS/PAA and PAA

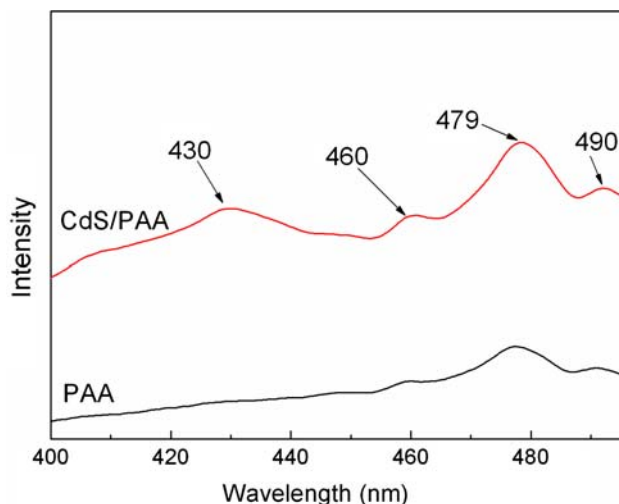


Fig. 7 PL spectra of CdS/PAA and PAA at 280 nm excitation wavelength

emission band centered at 430 nm is displayed on the PL spectra, which should be related to CdS. It was reported that the recombination of excitons and/or shallowly trapped electron/hole pairs causes the band edge luminescence. The PL emission indicates that, after light absorption in the CdS crystals, the photogenerated electron/hole pair was trapped, with emission at 430 nm upon their recombination [24, 25]. We believe that nanowires with high ratios (length/diameter) should have more surface and subsurface defects. Therefore, it is reasonable to believe that the PL from the CdS nanowires in our work can be attributed to the above-mentioned surface states. The PL band centered at 460, 479, and 490 nm originated from defects PL for PAA. After filled CdS into the pore channels, the PL intensity is obviously enhanced. This is probably caused from the fact that Cd^{2+} diffuses and enters the alumina template, resulting in the enhanced defects luminescence. The mechanism needs to be further researched in the future.

Summary

In summary, we report the preparation of CdS nanowires using nano-sized porous alumina template by the paired cell method. The nucleic and growth mechanism of CdS nanowires were investigated in detail. The results indicated the electrostatic adsorption and ions diffusion play the most important roles during the reaction process. The absorption edge in UV–Vis spectrum of CdS/PAA nanoarray shows blue shift due to the quantum confinement effects. The strong visible emission band of CdS nanocrystal centered at 430 nm provides the potential application of luminescence materials. Compared with other techniques, the present method not only shows the advantages of

simplicity, high efficiency, and low cost, but also possesses a potential for fabricating the other compound nanowires.

Acknowledgements This work was supported by the Key Item for Basic Research of Shanghai, China (Grant No.08JC1419000) and National Natural Science Foundation of China (Grant No.50672069).

References

1. Cao BL, Jiang Y, Wang C, Wang WH, Wang LZ, Niu M, Zhang WJ, Li YQ, Lee ST (2007) *Adv Funct Mater* 17:1501
2. Peng HL, Xie C, Schoen DT, McIlwrath K, Zhang XF, Cui Y (2007) *Nano Lett* 7:3734
3. Duan XF, Huang Y, Agarwal R, Lieber CM (2003) *Nature* 421:241
4. Greytak AB, Barrelet CJ, Li Y, Lieber CM (2005) *Appl Phys Lett* 87:151103
5. Ma RM, Dai L, Huo HB, Xu WJ, Qin GG (2007) *Nano Lett* 7:3300
6. Lin YF, Song JH, Ding Y, Lu SY, Wang ZL (2008) *Appl Phys Lett* 92:022105
7. Li Y, Wan J, Gu Z (2000) *Mater Sci Eng A* 286:106
8. Shi HQ, Zhou XD, Xun F, Wang DB, Hu ZS (2006) *Mater Lett* 60:1793
9. Kang CC, Lai CW, Peng HC, Shyue JJ, Chou PT (2007) *Small* 3:1882
10. Wang YW, Meng GW, Zhang LD, Liang CH, Zhang J (2002) *Chem Mater* 14:1773
11. Lin YF, Song JH, Ding Y, Lu SY, Wang ZL (2008) *Adv Mater* 20:3127
12. Routkevitch D, Bigioni T, Moskovits M, Xu JM (1996) *J Phys Chem* 100:14037
13. Xu DS, Shi XS, Guo GL, Gui LL, Tang YQ (2000) *J Phys Chem B* 104:5061
14. Li Y, Liao H, Fan Y, Li L, Qian Y (1999) *Mater Chem Phys* 58:87
15. Piao Y, Lim H, Chang JY, Lee WY, Kim H (2005) *Electrochim Acta* 50:2997
16. Piao Y, Kim H (2003) *Chem Commun* 2898
17. Masuda H, Fukuda K (1995) *Science* 268:1466
18. Huczko A (2000) *Appl Phys A* 70:365
19. Cortes A, Gómez H, Marotti RE, Riveros G, Dalchiale EA (2004) *Sol Energy Mater Sol Cells* 82:21
20. Guillén C, Martínez MA, Maffiotte C, Herrero J (2001) *J Electrochem Soc* 148:G602
21. Ikeda O, Ohtani M, Yamaguchi T, Komura A (1998) *Electrochim Acta* 43:833
22. Zhang HM, Zou KS, Li SH, Cui Y, Zhong HJ (2004) *J Funct Mater (Sup)* 35:2704
23. Mondal SP, Das K, Dhar A, Ray SK (2007) *Nanotechnology* 18:095606
24. Spanhel L, Anderson MA (1990) *J Am Chem Soc* 112:2278
25. Gao N, Guo F (2006) *Mater Lett* 60:3697